Enhanced Atrazine Degradation Using Laccase Immobilized on Arginine-Functionalized Boron Nitride Nanosheets

Yifan Gao[1], Minhao Xiao[1], Haiyuan Zou[2], Glenn Nurwono[2], David Zgonc[1], Junyoung O. Park[3], Jens Blotevogel[4], Chong Liu[2], Eric M.V. Hoek[1], Shaily Mahendra[*1]

[1]*Department of Civil and Environmental Engineering, University of California, Los Angeles, 580 Portola Plaza, Los Angeles, California, 90095, USA*

[2]*Department of Chemistry and Biochemistry, University of California, Los Angeles, 607 Charles E. Young Drive East, Los Angeles, California, 90095, USA*

[3]*Department of Chemical and Biomolecular Engineering, University of California, Los Angeles, 5531 Boelter Hall, Los Angeles, CA 90095, USA*

[4]*CSIRO, Environment, Waite Campus, Urrbrae, SA 5064, Australia*

Corresponding author: Department of Civil and Environmental Engineering, University of California, Los Angeles, CA 90095, United States. *E-mail:* mahendra@seas.ucla.edu (S. Mahendra)

https://doi.org/10.26434/chemrxiv-2024-lqj0v **ORCID:** https://orcid.org/0000-0002-4821-795X Content not peer-reviewed by ChemRxiv. **License:** CC BY 4.0

Abstract

Fungal enzyme-mediated systems have been widely employed for the degradation of environmental contaminants. However, the use of free enzymes is limited by the rapid loss of their catalytic activity, stability, and reusability, which further restricts their catalytic performance. In this work, we developed an enzyme immobilization platform by elaborately anchoring the fungal laccase onto arginine-functionalized boron nitride nanosheets (BNNS-Arg@Lac). BNNS-Arg@Lac showcased enhanced stability against fluctuating pH values and temperatures, along with remarkable reusability across six consecutive cycles, outperforming free natural laccase (nlaccase). As a demonstration, a model pollutant of atrazine (ATR) was selected for proof-of-concept applications, given substantial environmental and public health concerns in agriculture runoff. By applying BNNS-Arg@Lac, the ATR degradation rate was nearly doubled that of nlaccase. Moreover, BNNS-Arg@Lac consistently demonstrated superior ATR degradation capabilities in synthetic agricultural wastewater and various mediator systems compared to nlaccase. Comprehensive product analysis unraveled distinct degradation pathways for BNNS-Arg@Lac and nlaccase, further elucidating the mechanism of the laccase-catalyzed ATR treatment. Overall, this research provides a foundation for the future development of enzymatic catalysts in tackling pollution problems and may unlock new potential for green and efficient environmental remediation and waste management strategies.

Keywords: *Herbicide, fungi, nanomaterials, bioremediation, biocatalysis*

Synopsis: Laccases on arginine-functionalized boron nitride nanosheets showcase improved enzyme stability and atrazine degradation, advancing enzyme-nanomaterial hybrids for environmental cleanup.

https://doi.org/10.26434/chemrxiv-2024-lqj0v **ORCID:** https://orcid.org/0000-0002-4821-795X Content not peer-reviewed by ChemRxiv. **License:** CC BY 4.0

1. Introduction

Fungal enzymes, such as laccases, peroxidases, and cytochrome P450s, have been increasingly recognized for their significant role in the biodegradation of xenobiotics.[1–3] Among these enzymes, laccases have attracted growing attention in the bioremediation study due to their high reactivity and substrate versatility. Yet, a major setback of applying free laccase is the fast loss of enzymatic catalytic performance and stability when encountering environmental factors such as varied pH and fluctuating temperatures.[4] To address that, the enzyme immobilization technique has been employed, which entails attaching, crosslinking, or entrapping enzymes onto a solid substrate or within a porous support matrix.[2] Undergoing immobilization is expected to render several advantages over free laccases: (1) improved tolerance to harsh environmental conditions, including extreme temperatures and pH levels;[5] (2) easy recovery of enzymes from treated wastewater or contaminated sites;[6] (3) retained and augmented catalytic ability for targeted compound degradation.[7] To successfully synthesize powerful immobilized laccases, selecting the appropriate supporting materials is a crucial aspect.[8]

We envision that boron nitride nanosheets (BNNSs), also known as “white graphene”, are promising for laccase immobilization. BNNSs consist of a few atomic thickness layers of bulk hexagonal boron nitride (hBN)[9] and resemble structures of graphene, with B atoms and N atoms substituting for C atoms. BNNSs offer several advantages for enzyme immobilization and environmental applications. BNNSs showed higher surface areas than hBN (BNNSs: ~2,600 $m^2 g^{-1}$; bulk hBN: ~10 $m^2 g^{-1}$).[10] Additionally, the remarkable chemical stability of BNNSs makes them suitable for use in a wide range of environments.[11,12] Their high biocompatibility[13] reduces concerns of secondary contamination. In order to enable better enzyme attachment on BNNSs, the exfoliation and functionalization process during the BNNSs

https://doi.org/10.26434/chemrxiv-2024-lqj0v ORCID: https://orcid.org/0000-0002-4821-795X Content not peer-reviewed by ChemRxiv. License: CC BY 4.0

synthesis is necessary for increasing BNNSs solubility and providing covalent binding positions. One promising method is using amino acids to facilitate the process. Amino acids can interact with boron nitride via covalent bonds (Lewis acid-base between N atom and hydrophilic carboxylic group) and van der Waals forces (π–π interaction between R groups).[14,15] The combination of amino acids can increase the dispersion of BNNSs in water[24] and provide functional groups (amine group) at the same time.[14,16] Therefore, it is logical to propose that amino-acid functionalized BNNSs can serve as a representative platform to immobilize laccase, which can be further used in environmental remediation efforts.

As an extensively used herbicide, atrazine (ATR) has drawn our attention as a model contaminant. The wide usage of ATR over the years for controlling broadleaf weeds in commercial crops has resulted in its accumulation in soils, groundwater, and crops.[17,18] Given its role as an endocrine disruptor and its carcinogenic potential,[18–21] the presence of ATR leads to enduring environmental concerns. Many approaches for ATR elimination have been deployed, such as physicochemical (e.g. adsorption), chemical (e.g. Fenton/Fenton-like reactions, electrochemical, and photocatalysis), and biological solutions.[17,22–25] Under the umbrella of biological methods, laccases can catalyze reactions that are responsible for ATR degradation. For example, plant laccases as oxidases have shown to be capable of oxidizing the ethyl side of ATR.[26] Fungal laccases generally have high redox potential which makes them more favorable than plant or bacterial laccases.[2] Nevertheless, little is known about detailed studies of fungal laccase-mediated ATR degradation systems and underlying mechanisms. Therefore, ATR serves as an ideal model contaminant for understanding the environmental implication of BNNSs immobilized laccases.

https://doi.org/10.26434/chemrxiv-2024-lqj0v **ORCID:** https://orcid.org/0000-0002-4821-795X Content not peer-reviewed by ChemRxiv. **License:** CC BY 4.0

To fill these knowledge gaps, we synthesized an enzyme-catalyst involving immobilized laccase onto amino acid functionalized BNNSs and investigated its ability to degrade ATR. Laccase was immobilized on arginine-functionalized BNNSs (BNNS-Arg). We assessed the performance of the resulting catalyst, BNNS-Arg@Lac, in degrading ATR across a range of simulated water chemistries and compared it with natural laccase (nlaccase). The comprehensive degradation pathways have also been proposed. This work demonstrated that BNNS-Arg@Lac holds significant potential to be applied in natural and engineered environments for contamination treatment.

2. Materials and Methods

Materials and Chemicals. Bulk hexagonal boron nitride powder (hBN) was purchased from MSE Supplies. All chemicals were purchased from Thermo Fisher Chemical or Sigma Aldrich unless otherwise stated. Crude laccase extract from *Pycnoporus sp. SYBC-L3*[27,28] was gifted by Dr. Qingguo Huang, University of Georgia.

Synthesis of amino acid-functionalized BNNSs. Amino acids, arginine (Arg), tryptophan (Trp), cysteine (Cys), aspartic acid (Asp), and Serine (Ser), were selected based on their different R-side chain properties. Different amino acids (1.5 g) were dissolved in deionized (DI) water (15 mL) at 50 °C for 10 min. Then, 0.5 g bulk hBN powder was added to each amino acid solution, followed by 4-h ultrasonication (Thermo Fisher, 40 kHz). All post-ultrasonicated samples were centrifuged at 2,000 rpm for 5 min. The supernatant was then filtered by 0.2 μm nylon membrane, washed with 100 mL DI water, and oven-dried at 60 °C. Different mass ratios of hBN powder:amino acids and different ultrasonication times were also examined for optimization. Finally, BNNSs functionalized by Arg (BNNS-Arg) were selected.

https://doi.org/10.26434/chemrxiv-2024-lqj0v **ORCID:** https://orcid.org/0000-0002-4821-795X Content not peer-reviewed by ChemRxiv. **License:** CC BY 4.0

Preparation of activated BNNS-Arg. To activate BNNS-Arg by N-ethyl-N′-(3-(dimethylamino)propyl)carbodiimide /N-hydroxysuccinimide (EDC/NHS) crosslinking system, 100 mg BNNS-Arg was added into 10 mL 2-(N-morpholino)ethanesulfonic acid (MES) buffer (pH 6). The ratio of 2:1 of EDC:NHS was then added (0.1 g EDC + 0.05 g NHS per 10 mL solution), followed by continuous stirring at room temperature for 4 h. The solution was filtered, washed, and dried. The dry powder was collected for further immobilization experiments.

Laccase immobilization on activated BNNS-Arg (BNNS-Arg@Lac). One mL purified natural laccase (nlaccase) (purified method in **supporting information**) was mixed with 100 mg EDC/NHS-activated BNNS-Arg in 10 mL 0.1 M Na-PO_4 buffer (pH 3). The solution was stirred overnight at 30 °C, collected, and then vacuum-filtered. The solid sample was washed with DI water for non-immobilized nlaccase and dried at room temperature in the fume hood. After that, the generated BNNS-Arg@Lac activity was analyzed by 2,2'-azino-bis(3-ethylbenzothiazoline-6-sulfonic acid) (ABTS) assay (see **supporting information**). The process of synthesizing BNNS-Arg@Lac was shown in **Figure 1A**.

Characterization methods. The morphology of bulk BN powder, BNNS-Arg, and BNNS-Arg@Lac was characterized by scanning electron microscope (SEM; Phenom Pharos G2 Desktop FEG-SEM, Thermo Fisher), transmission electron microscopy (TEM; FEI Tecnai T12, Tecnai), and high-resolution transmission electron microscopy (HRTEM; Talos F200C G2, Thermo Fisher). For SEM samples, all materials were dried and sputter-coated with Pt. TEM and HRTEM samples were resuspended in ethanol and dried on Lacey carbon support. The elements on the material surfaces were detected by SEM equipped with an energy dispersive X-ray detector (EDS) (Phenom Pharos G2 Desktop FEG-SEM, Thermo Fisher). The detailed structures were studied by X-ray diffraction (XRD; D8 Discover Powder X-ray Diffractometer; Bruker),

https://doi.org/10.26434/chemrxiv-2024-lqj0v **ORCID:** https://orcid.org/0000-0002-4821-795X Content not peer-reviewed by ChemRxiv. **License:** CC BY 4.0

Fourier transform infrared microscopy (FTIR; Nicolet™ iS™ 10 FTIR Spectrometer, Thermo Fisher), and X-ray photoelectron spectroscopy (XPS).

Evaluation of pH stability, thermal stability, and reusability of BNNS-Arg@Lac. The catalytic ability to oxidize ABTS was used to evaluate the pH stability, thermal stability, and reusability of BNNS-Arg@Lac. BNNS-Arg@Lac and natural laccase were incubated in ABTS solutions with pH values ranging from 2.5 to 7. The relative activities at various pH values were normalized to activities at their optimum pH (pH 3). To determine the thermal stability, temperatures from 20 °C to 70 °C were utilized and both BNNS-Arg@Lac and natural laccase were incubated at certain temperatures for 10 hours. For the reusability test, 20 mg of BNNS-Arg@Lac was incubated with 2 mM ABTS and reused by high-speed centrifugation (20,000 g). Then the pellets were resuspended into fresh 2 mM ABTS solution to start a new catalytic cycle.

Atrazine degradation catalyzed by BNNS-Arg@Lac. All degradation experiments were conducted in 250 mL Erlenmeyer flasks at 30 °C, 120 rpm, containing 50 mL Na-PO_4 buffer (pH 3), 10 mg/L ATR, and 150 U/L nlaccase and BNNS-Arg@Lac (20 μM mediator or synthetic agricultural water). The initial ATR concentration was selected based on previously reported studies.[29–32] For sampling, 500 μL samples were extracted and filtered through 0.22 μm filters. After mixing with acetonitrile (1:1, v/v), filtered samples were analyzed by high-pressure liquid chromatography (HPLC, Thermo Fisher) with a ZORBAX Eclipse Plus C18 column (150 mm × 4.6 mm, 5 μm, Agilent) and a UV detector at 220 nm. The analytic method was based on previous work:[29] Under isocratic conditions, the mobile phase was acetonitrile:water at 50:50 with a flow rate of 0.6 mL/min. The inhibition effects of chlorophyll a synthesis in model algal strain, *Chlorella vulgaris* was performed for detoxication study (see **supporting information**).

https://doi.org/10.26434/chemrxiv-2024-lqj0v **ORCID:** https://orcid.org/0000-0002-4821-795X Content not peer-reviewed by ChemRxiv. **License:** CC BY 4.0

Analytical identification of degradation products. Samples were taken at 0, 4, 8, 12, and 24 h for intermediates and end-product analysis. In general, 500 µL samples were first 0.22 µm filtered. Next, filtered samples containing enzymes were injected through Zeba™ Spin Desalting Columns (7K MWCO, Thermo Fisher), and elutes were saved. Then samples were analyzed using LC/MS-QTOF (Agilent 6545) for product identification based on their mass-to-charge ratio (m/z) (details in **supporting information)**.

3. Results and Discussion

Synthesis and Characterization. We proposed a single-step exfoliation and functionalization of BNNS using the amino acids-assisted ultrasonication method. A variety of amino acids with different side chain structures (Arg: positively charged; Trp: hydrophobic; Cys: S-containing; Asp: negative charged; Ser: polar uncharged) were tested. Different from previously reported work,[14] instead of Trp, Arg showed higher BNNS dispersion, yield, and stable solubility in water (**Figure S1**). The more efficient exfoliation could be both the more favorable adsorption energy between Arg analog and boron nitride nanomaterials through π-stacking interactions, based on the theoretical calculation,[33] and a much higher solubility of Arg than Trp at the same concentration. Therefore, after the optimization of Arg: bulk hBN ratio and ultrasonication time (see **Table S1**), we proceeded with Arg for the following BNNS synthesis to form BNNS-Arg.

After synthesis, the morphology as prepared BNNS-Arg and bulk hBN were examined by scanning electron microscopy (SEM), transmission electron microscopy (TEM), and high-resolution transmission electron microscopy (HRTEM). Under SEM (**Figure 1B** and **1E**), BNNS-Arg showed reduced size (~0.1 µm) and thickness (~1 nm) compared to bulk hBN (size: ~1.5 µm; thickness: ~60 nm). As shown in **Figure 1C** and **1F**, the TEM images presented that after arginine facilitated exfoliation and function, BNNS-Arg exhibited 2D structure as well as

https://doi.org/10.26434/chemrxiv-2024-lqj0v **ORCID:** https://orcid.org/0000-0002-4821-795X Content not peer-reviewed by ChemRxiv. **License:** CC BY 4.0

fewer layers compared to bulk hBN. The thinner structure of BNNS-Arg was further confirmed by HRTEM results (**Figure 1D** and **1G**). The contrast of bulk hBN to the background was higher than BNNS-Arg, which showed the thicker nature of bulk hBN. These results demonstrated the effective BNNS exfoliation. After laccase immobilization, formed BNNS-Arg@Lac still presented the same morphology as BNNS-Arg, which confirmed the nanosheet structure of our catalysts. Moreover, element mapping has been conducted to verify the successful linkage between laccase and BNNS-Arg, for BNNS-Arg only B, N, C, and O were observed on the surface (**Figure S2**). However, in addition to these elements, laccase-exclusive elements: Cu and S were also observed on BNNS-Arg@Lac, which demonstrated laccase has been loaded on the BNNS-Arg surface (**Figure 1H-N**).

https://doi.org/10.26434/chemrxiv-2024-lqj0v **ORCID:** https://orcid.org/0000-0002-4821-795X Content not peer-reviewed by ChemRxiv. **License:** CC BY 4.0

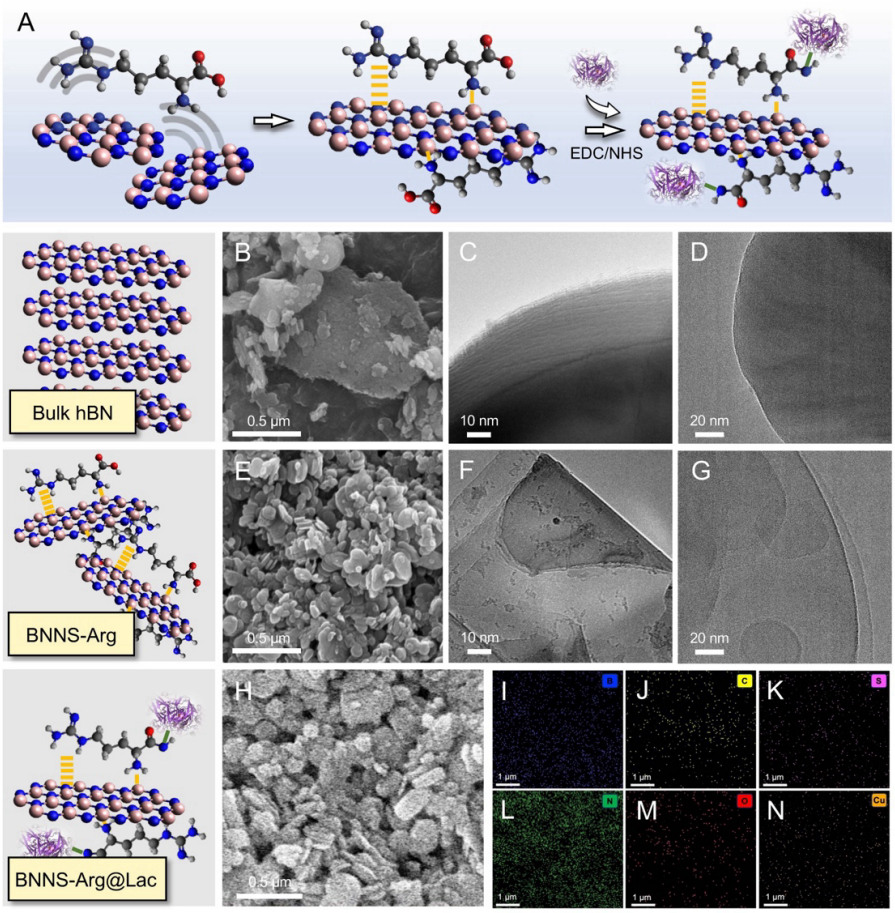

Figure 1. Synthesis and structure characterization of BNNS-Arg@Lac. (A) Schematic illustration (not to scale) of the synthesis of BNNS-Arg@Lac. (B, E, and H) SEM images of bulk hBN, BNNS-Arg, and BNNS-Arg@Lac. (C and F) TEM images of bulk hBN and BNNS-Arg. (D and G) HRTEM images of bulk hBN and BNNS-Arg. (I-N) EDS mapping of BNNS-Arg@Lac.

To further uncover the structural information and successful laccase immobilization of BNNS-Arg@Lac, the XRD analysis, FTIR, and XPS were performed. As shown in **Figure 2A**, two characteristic diffraction peaks were observed at 26.7° and 42.1° for both BNNS-Arg and BNNS-Arg@Lac, which is ascribed to the (111) and (200) face of boron nitrite, implying the arginine decoration and the subsequent laccase immobilization process of laccase did not change the host structure.[15] From the FTIR, the fingerprint bonds of B-N stretching (1370 cm^{-1}) and B-N

https://doi.org/10.26434/chemrxiv-2024-lqj0v **ORCID:** https://orcid.org/0000-0002-4821-795X Content not peer-reviewed by ChemRxiv. **License:** CC BY 4.0

bending (820 cm^{-1}) can be observed in all BNNS-contained samples, which is contributed by the boron nitride substrate.[16] The liquid nlaccase sample revealed C-O-C stretching (1099 cm^{-1}), CONH peptide linkage (1630 cm^{-1}), and an abundant O-H stretching peak that was contributed by H_2O.[34] Both BNNS-Arg and BNNS-Arg@Lac exhibited peaks corresponding to C-N bonds, O-H bending vibration of carboxyl groups, and C-O bonds, which overlapped with B-N stretching peaks (1370 cm^{-1}). Owing to the addition of laccase, more C-N, O-H bending, and C-O peaks presented in BNNS-Arg@Lac, leading to a greater reduction of B-N stretching peaks. It could be due to the coverage of laccase on the BNNS-Arg surface. Another evidence of nlaccase immobilized on BNNS-Arg was the observation of signature peaks of nlaccase: C-O-C stretching and CONH peptide linkage, in BNNS-Arg@Lac samples. Further chemical state and composition were identified by the XPS. Illustrated in **Figure 2C**, the XPS survey shows the presence of B 1*s*, C 1*s*, N 1*s*, and O 1*s* signals in both samples, which can be attributed to the incorporation of arginine within BNNS-Arg and additional amino acids in BNNS-Arg@Lac. Notably, the deconvoluted C1s spectra (**Figure 2D**) showed the difference in prominent bonds, C-C (sp2), C-O/C-N, and C=O. The BNNS-Arg@Lac spectra exhibited peak area ratios of 28:20:15 for C-C, C-O/C-N, and C=O respectively, aligning with the typical bond ratios found in laccase's chemical architecture.[35,36] Given the XPS surface detection limit and larger molecule size, laccase should represent the primary composition detected if it covered the surface.[34] The peak emergence concurs with the anticipated bond chemistry inherent to the enzyme's structure. BNNS-Arg spectra indicated a diminution in the peak area ratio of C-O/C-N relative to C-C but with a similar ratio of C-C to C=O as arginine. It was likely due to the grafting of periphery arginine's C-O and C-N bonds onto the BNNS during exfoliation while C-C and C=O bonds were still detectable.[14] Further, as shown in **Figure S3**, deconvolution of N1*s* spectra revealed

https://doi.org/10.26434/chemrxiv-2024-lqj0v **ORCID:** https://orcid.org/0000-0002-4821-795X Content not peer-reviewed by ChemRxiv. **License:** CC BY 4.0

peaks corresponding to B-N and N-H, indicative of the BNNS bone structures. Despite the low abundance of Cu and S in laccase (**Figure S4-S5**), which resulted in no significant peaks for these elements, the observations were consistent with XPS spectral expectations.

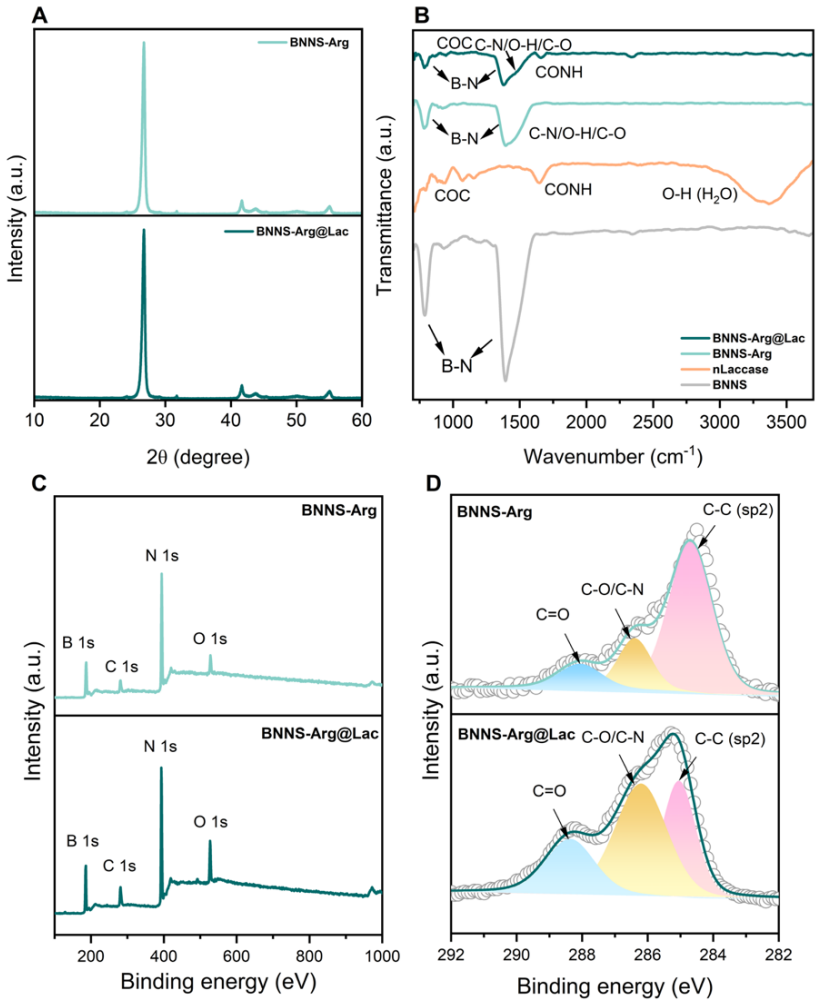

Figure 2. Structure analysis of BNNS-Arg@Lac. (A) XRD spectra of BNNS-Arg and BNNS-Arg@Lac. B: FTIR spectra of BNNS-Arg and BNNS-Arg@Lac. (C) XPS spectra of BNNS-Arg and BNNS-Arg@Lac. (D) Deconvoluted XPS spectra of C1*s* in BNNS-Arg and BNNS-Arg@Lac.

Stability and Reusability of BNNS-Arg@Lac. Environmental factors, such as fluctuations in pH and temperature, can compromise the stability of enzymes. Consequently, we tested and compared both nlaccase and BNNS-Arg@Lac catalytic ability towards ABTS across a wide

https://doi.org/10.26434/chemrxiv-2024-lqj0v **ORCID:** https://orcid.org/0000-0002-4821-795X Content not peer-reviewed by ChemRxiv. **License:** CC BY 4.0

range of pH levels and temperatures. As illustrated in **Figure 3A**, both laccases showed optimal performance at a pH of 3. However, at conditions approaching a neutral pH, BNNS-Arg@Lac retained more activity, whereas natural laccase nearly lost all its activity when the pH was adjusted to 5.5. Given that most environmentally relevant reactions occur around 15 °C, the stability of enzymatic catalysts at these mild temperatures is crucial. We assessed the performance of the two laccase forms across a temperature range of 20 °C to 70 °C (**Figure 3B**). Within this mild temperature range, BNNS-Arg@Lac showcased the highest enzyme activity, underscoring its adaptability to natural conditions. In line with previous studies,[37] nlaccase peaked in activity at 50 °C, but it is not an environmentally relevant condition. The enhanced stability in the face of changing natural conditions can likely be attributed to the interaction between laccase and arginine on BNNS. Many studies indicate that the covalent modification of enzymes with small molecules, such as natural amino acids, can bolster their stability.[38,39] Thus, arginine might not only aid in the synthesis of the supporting material, BNNS, but also enhance the stability of the immobilized enzymes.

The recyclability of BNNS-Arg@Lac has been evaluated through continuous separation and dispersion across multiple reaction cycles (**Figure 3C**). The secure peptide binding of laccase to BNNS-Arg minimizes potential leakage during separation, enhancing the reusability of BNNS-Arg@Lac, which was supported by previous research that reported a similar immobilization strategy.[40] This high reusability could also potentially reduce the cost of our catalyst, BNNS-Arg@Lac, further showing the outperformance of this immobilization approach.[40]

https://doi.org/10.26434/chemrxiv-2024-lqj0v **ORCID:** https://orcid.org/0000-0002-4821-795X Content not peer-reviewed by ChemRxiv. **License:** CC BY 4.0

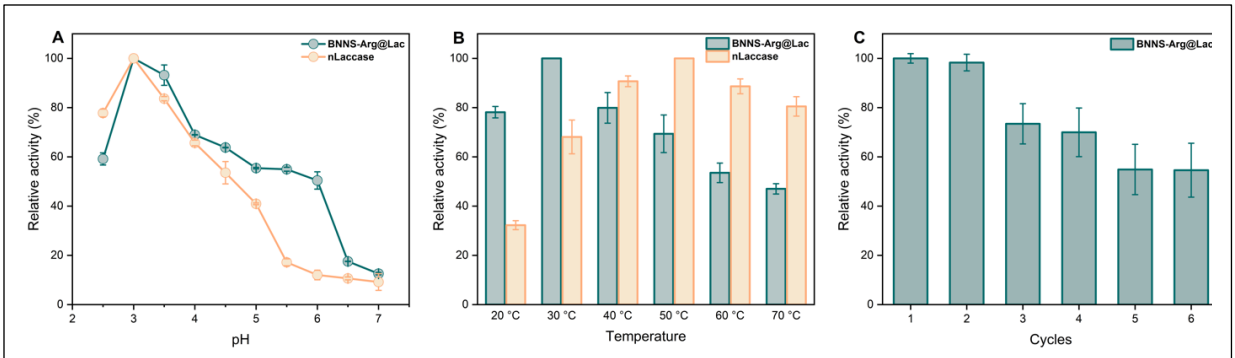

Figure 3. Stability and reusability study of BNNS-Arg@Lac and nlaccase. (A) Relative activity across pH ranges from 2.5 to 7, normalized to their activities at the optimal pH. (B) Thermal stability from 20 C to 70 °C, normalized to their activities at the optimal temperatures. (C) Reusability evaluation of BNNS-Arg@Lac after 6 consecutive cycles. Error bars represent the standard deviation of the means (n = 3).

Enhanced Degradation of Atrazine by BNNS-Arg@Lac. The ATR degradation reaction system was first established under laboratory conditions in a 0.1 M Na-PO_4 buffer at pH 3 and 30 °C to achieve better performance of catalysts. Within 24 h, BNNS-Arg@Lac showed ~69% of ATR degradation while nlaccase only showcased ~35% of ATR concentration reduction (**Figure 4A**). In abiotic control and inactive laccase control (**Figure S6**), ATR did not exhibit significant change. In the BNNS-Arg group, ATR concentration showed a slight reduction (~12%). This decrease might be ascribed to the partial ATR adsorption on the BNNS-Arg backbone. ATR has an electron lone pair on the N atom, which can be considered as a Lewis base. B on BNNS has a positive charge which can be leveraged as Lewis acid.[12] The Lewis acid-base interaction that occurred between ATR and BNNS-Arg backbone caused adsorption. The adsorbed ATR is likely to have increased access to the active centers of laccases on BNNSs, as the diffusion resistance between the bulk solution and the laccases can be mitigated by the synergistic effect of substrate adsorption.[41] In addition, the enhanced stability of laccase after

https://doi.org/10.26434/chemrxiv-2024-lqj0v ORCID: https://orcid.org/0000-0002-4821-795X Content not peer-reviewed by ChemRxiv. License: CC BY 4.0

immobilization may further enhance the ATR catalyzation by retaining the microenvironment of the active sites.[42] Altogether, the overall ATR degradation was raised compared to nlaccase.

Correspondingly, two predominant intermediates have been tentatively identified: hydroxyatrazine with an m/z of 198.13 and cyanuric acid with an m/z of 130.07 (**Figure 4B**).[29,43] From the initial timepoint (0 h), BNNS-Arg@Lac group has produced a higher level of hydroxyatrazine and faster production of cyanuric acid than nlaccase group. This result implied BNNS-Arg@Lac catalyzes ATR with a higher turnover rate. In addition, the observation aligned with previous reports of enzyme inhibition by ATR and similar s-triazine derivatives in human liver microsomes.[44] Therefore, the disparity in degradation results could also stem from the product inhibition on nlaccase by other intermediates formed during ATR degradation.

Next, we tested various common mediators in laccase-mediated reactions for degrading ATR, namely 1-hydroxybenzotriazole (HBT), 2,2,6,6-Tetramethylpiperidine 1-oxyl (TEMPO), guaiacol (GA), and syringaldehyde (SA). Mediators are a class of compounds that can be oxidized by laccase into intermediates early in the reaction, which then react with the non-phenolic groups of the substrates.[2] Of the four mediators examined, the HBT group in the BNNS-Arg@Lac system achieved the highest ATR removal (~96%), followed by GA (~52%), SA (~10%), and TEMPO (~5%). nLaccase showed the same order for ATR removal efficiency (HBT>GA>SA>TEMPO). However, even with the addition of mediators, nlaccase mostly showed a lower reduction in ATR concentration. By adding only HBT, ATR and HBT can also conjugate together, decreasing the ATR concentration (**Figure S7**).[45] Although mediators like HBT can improve ATR degradation (for example for BNNS-Arg@Lac, with HBT, an ~96% degradation rate was achieved versus ~69% without it), the addition of HBT caused toxicity to chlorophyll a synthesis in the model organism, *C. vulgaris* (**Figure S8**). ATR, HBT, and their

https://doi.org/10.26434/chemrxiv-2024-lqj0v **ORCID:** https://orcid.org/0000-0002-4821-795X Content not peer-reviewed by ChemRxiv. **License:** CC BY 4.0

mixture all showed inhibition to chlorophyll a synthesis compared with the control group in normal algal growth. Conversely, chlorophyll a synthesis was not significantly impacted when treated with BNNS-Arg@Lac and natural laccase in the presence of HBT, suggesting that they can alleviate the inhibitory effects of HBT. Nonetheless, mediators can complicate the degradation system and pose potential environmental concerns for practical applications.

To further assess the practical potential of BNNS-Arg@Lac in more environmentally relevant conditions, experiments for ATR degradation were set up in prepared synthetic agricultural wastewater according to previous work[46,47] (see **supporting information** for recipe). High levels of nitrogen and phosphorus characterize agricultural runoff.[47,48] These elements are known to inhibit the activity of certain enzymes in the soil.[49] Thus, the investigation of BNNS-Arg@Lac performance in a more complex reaction system is important for its practical deployment. As illustrated in **Figure 4D**, BNNS-Arg@Lac still maintained superior ATR degradation performance compared to nlaccase. Yet, ATR degradation was still inevitably reduced, possibly due to the inhibitory effects of complex components on laccase activities. Collectively, our results endorsed BNNS-Arg@Lac as a more efficient catalyst for ATR degradation, even in conditions that closely mirror environmental scenarios.

https://doi.org/10.26434/chemrxiv-2024-lqj0v **ORCID:** https://orcid.org/0000-0002-4821-795X Content not peer-reviewed by ChemRxiv. **License:** CC BY 4.0

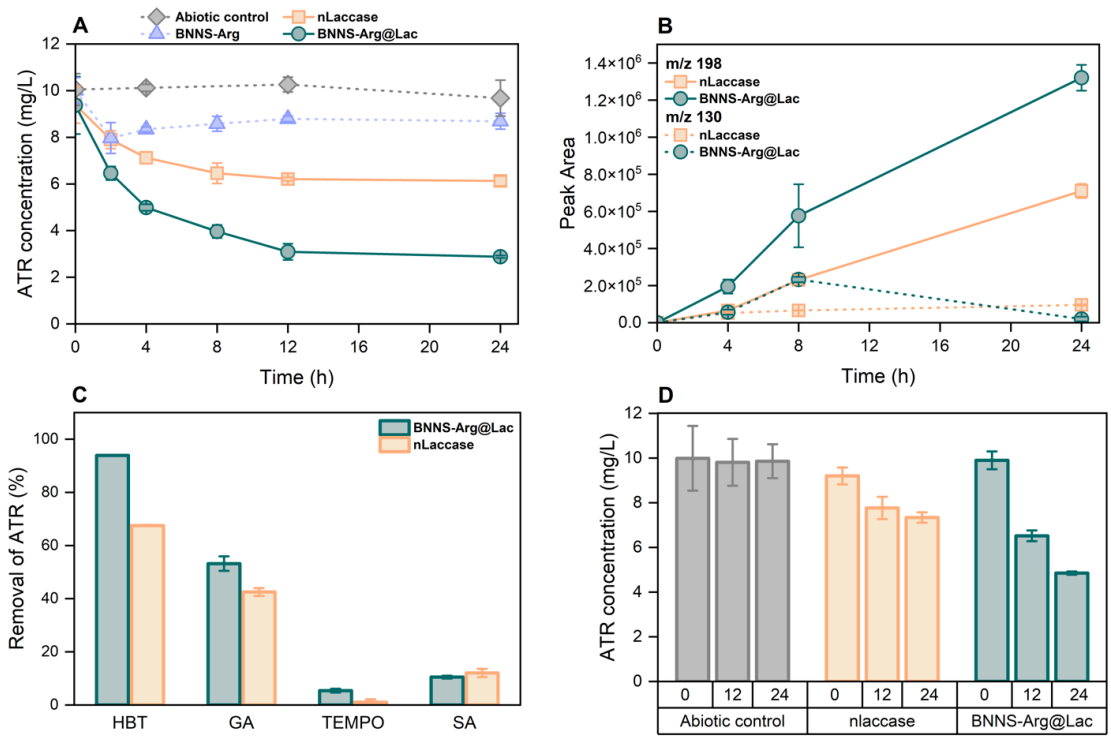

Figure 4. Degradation of ATR by BNNS-Arg@Lac and nlaccase. (A) ATR parent compound degradation by BNNS-Arg@Lac and nlaccase. Control groups included abiotic control and BNNS-Arg adsorption group. (B) Formed products at m/z 198 and 130 by BNNS-Arg@Lac and nlaccase. (C) ATR degradation by BNNS-Arg@Lac and nlaccase with different commonly used mediators. (D) ATR degradation by BNNS-Arg@Lac and nlaccase in synthetic agricultural wastewater, sampling at 0, 12, and 24 h.

Proposed Biodegradation Pathways by nLaccase and BNNS-Arg@Lac. For ATR biodegradation, we observed the distinct pathways during nlaccase and BNNS-Arg@Lac catalyzed reactions (**Figure 5**). In nlaccase group, after 4 h, ATR ($C_8H_{14}ClN_5$) was presumably oxidized to $C_8H_{13}ClN_5OH$ and $C_8H_{13}ClN_5OH$ was further oxidized to $C_8H_{12}ClN_5(OH)_2$ at 12 h. At 8 h, we tentatively identified another intermediate ($C_8H_{14}N_5OH$) generated from the dechlorination reaction. Then this intermediate was oxidized to another two products: $C_3N_3(OH)_3$ and $C_3N_3H_3O_3$. After 12 h, no significant products were generated in nlaccase group. In contrast,

https://doi.org/10.26434/chemrxiv-2024-lqj0v ORCID: https://orcid.org/0000-0002-4821-795X Content not peer-reviewed by ChemRxiv. License: CC BY 4.0

in BNNS-Arg@Lac group, at 4 h, a dechlorination product, $C_8H_{14}N_5OH$, was putatively identified and then oxidization products $C_3N_3(OH)_3$ and $C_3N_3H_3O_3$ emerged in 8-h samples. At 12 h, smaller molecules: $C_4N_2H_6O_3$ and $C_2N_2H_3O_2$ were tentatively identified as products. More products, such as $C_4H_{12}N_4OCl$ were putatively identified at the first 4 h and $C_5H_8ClN_5$ appeared at 8 h and then was oxidized to $C_5H_6ClN_4OH$. The end product profiles at 24 h illustrated that the BNNS-Arg@Lac group resulted in the production of a greater number of smaller compounds compared to using only nlaccase. This difference in compound composition may explain why samples subjected to 24-hour BNNS-Arg@Lac catalysis exhibited lower toxicity towards chlorophyll a synthesis in *C. vulgaris* (**Figure S8**). Two models were proposed by molecular docking (**see supporting information and Figure S9**). ATR binding affinity with nlaccase was -5.3 kcal/mol. Because of the software limitation, the graphene-like nanosheet was used as the best representation of BNNSs.[50] After the docking, ATR binding affinity with the immobilized laccase was increased to -10.3 kcal/mol. The modeling result indicated that the change in enzyme structure might be responsible for the different ATR degradation outcomes.

https://doi.org/10.26434/chemrxiv-2024-lqj0v **ORCID:** https://orcid.org/0000-0002-4821-795X Content not peer-reviewed by ChemRxiv. **License:** CC BY 4.0

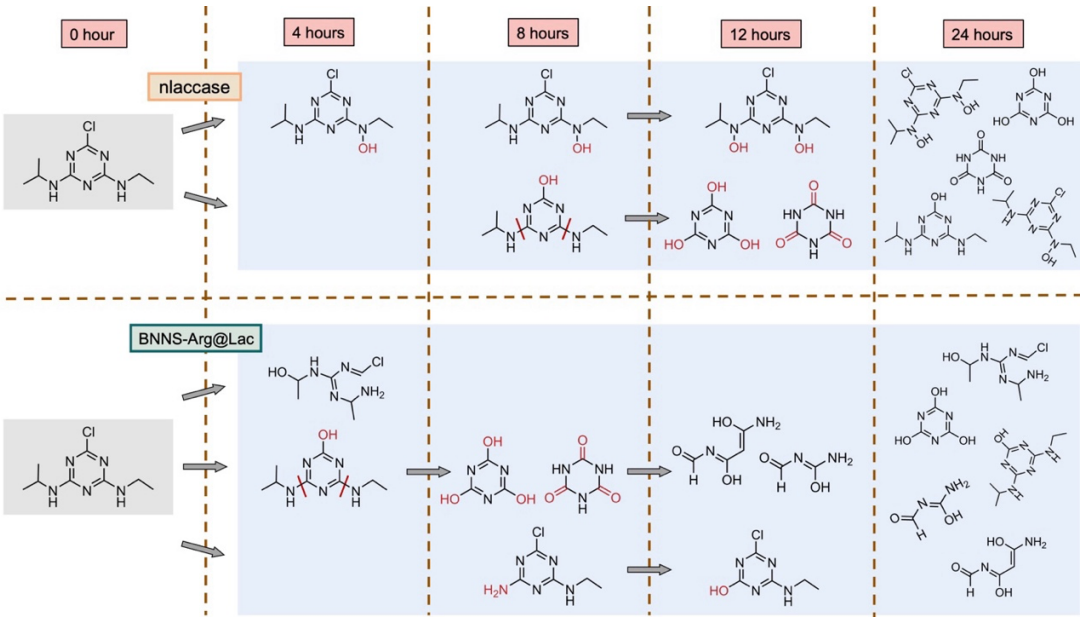

Figure 5. Proposed degradation pathways by BNNS-Arg@Lac and nlaccase. Intermediates and end products were analyzed at 4, 8, 12, and 24 h.

4. Environmental Implications

The use of ATR to protect (predominantly) corn crops in the U.S. creates significant human health and environmental risks;[51] we note that ATR is banned in the EU where it is manufactured.[52] Our catalyst, BNNS-Arg@Lac, showed high efficacy in ATR degradation as well as excellent stability and enhanced reusability (relative to nlaccase) even in a complex (synthetic) agricultural wastewater. The green synthesis process of BNNS-Arg did not require any toxic organic solvents and laccase is immobilized using natural peptide bonds. More importantly, BNNS-Arg@Lac overcame the traditional bottleneck of enzymatic catalysts, i.e., rapid decline in catalytic activity and stability in real environmental conditions. Unlike free enzymes, which are non-recoverable post-use, BNNS-Arg@Lac retains most of its efficacy upon reuse up to 6 cycles tested herein. The ATR degradation result of BNNS-Arg@Lac also reduced secondary contamination, making by-products less harmful. BNNS-Arg@Lac catalyzed ATR

https://doi.org/10.26434/chemrxiv-2024-lqj0v **ORCID:** https://orcid.org/0000-0002-4821-795X Content not peer-reviewed by ChemRxiv. **License:** CC BY 4.0

degradation generated smaller molecules and better detoxification ability than its free counterpart. Therefore, enzyme immobilization as demonstrated herein is a promising approach to expand the potential of enzymes while being produced via a green chemistry process.

Acknowledgment

The authors are grateful to Dr. Leonard H. Rome and Dr. David Jassby for their invaluable suggestions during the initial discussions. Our thanks also go to Jingyu Wang, Dr. Yongchao Xie, Randy Chen, Richard Law, and Emily Tieu for their assistance with the experimental work. We are thankful to Dr. Qingguo Huang for the generous gift of natural laccase. Lastly, we appreciate Dr. Yu Chen and Dr. Mallikarjuna Nadagouda's support in product analysis.

References

(1) Harms, H.; Schlosser, D.; Wick, L. Y. Untapped Potential: Exploiting Fungi in Bioremediation of Hazardous Chemicals. *Nat. Rev. Microbiol.* **2011**, *9* (3), 177–192.

(2) Gao, Y.; Shah, K.; Kwok, I.; Wang, M.; Rome, L. H.; Mahendra, S. Immobilized Fungal Enzymes: Innovations and Potential Applications in Biodegradation and Biosynthesis. *Biotechnol. Adv.* **2022**, *57* (February), 107936. https://doi.org/10.1016/j.biotechadv.2022.107936.

(3) Gao, Y.; Croze, B.; Birch, Q. T.; Nadagouda, M. N.; Mahendra, S. Sorghum-Grown Fungal Biocatalysts for Synthetic Dye Degradation. *Water Res. X* **2023**, *19* (March), 100181. https://doi.org/10.1016/j.wroa.2023.100181.

(4) Franssen, M. C. R.; Steunenberg, P.; Scott, E. L.; Zuilhof, H.; Sanders, J. P. M. Immobilised Enzymes in Biorenewables Production. *Chem. Soc. Rev.* **2013**, *42* (15), 6491–6533. https://doi.org/10.1039/c3cs00004d.

https://doi.org/10.26434/chemrxiv-2024-lqj0v **ORCID:** https://orcid.org/0000-0002-4821-795X Content not peer-reviewed by ChemRxiv. **License:** CC BY 4.0

(5) Maghraby, Y. R.; El-Shabasy, R. M.; Ibrahim, A. H.; Azzazy, H. M. E. S. Enzyme Immobilization Technologies and Industrial Applications. *ACS Omega* **2023**, *8* (6), 5184–5196. https://doi.org/10.1021/acsomega.2c07560.

(6) Andler, S. M.; Goddard, J. M. Transforming Food Waste: How Immobilized Enzymes Can Valorize Waste Streams into Revenue Streams. *npj Sci. Food* **2018**, *2* (1). https://doi.org/10.1038/s41538-018-0028-2.

(7) Bornscheuer, U. T. Immobilizing Enzymes: How to Create More Suitable Biocatalysts. *Angew. Chemie - Int. Ed.* **2003**, *42* (29), 3336–3337. https://doi.org/10.1002/anie.200301664.

(8) Zhu, Y.; Huang, Z.; Chen, Q.; Wu, Q.; Huang, X.; So, P. K.; Shao, L.; Yao, Z.; Jia, Y.; Li, Z.; Yu, W.; Yang, Y.; Jian, A.; Sang, S.; Zhang, W.; Zhang, X. Continuous Artificial Synthesis of Glucose Precursor Using Enzyme-Immobilized Microfluidic Reactors. *Nat. Commun.* **2019**, *10* (1), 1–9. https://doi.org/10.1038/s41467-019-12089-6.

(9) Qanbarzadeh, M.; DiGiacomo, L.; Bouteh, E.; Alhamdan, E. Z.; Mason, M. M.; Wang, B.; Wong, M. S.; Cates, E. L. An Ultraviolet/Boron Nitride Photocatalytic Process Efficiently Degrades Poly-/Perfluoroalkyl Substances in Complex Water Matrices. *Environ. Sci. Technol. Lett.* **2023**, *10* (8), 705–710. https://doi.org/10.1021/acs.estlett.3c00363.

(10) Rasul, M. G.; Kiziltas, A.; Arfaei, B.; Shahbazian-Yassar, R. 2D Boron Nitride Nanosheets for Polymer Composite Materials. *npj 2D Mater. Appl.* **2021**, *5* (1). https://doi.org/10.1038/s41699-021-00231-2.

(11) Zhou, X.; Kang, F.; Qu, X.; Fu, H.; Alvarez, P. J. J.; Tao, S.; Zhu, D. Role of Extracellular Polymeric Substances in Microbial Reduction of Arsenate to Arsenite by Escherichia Coli

https://doi.org/10.26434/chemrxiv-2024-lqj0v **ORCID:** https://orcid.org/0000-0002-4821-795X Content not peer-reviewed by ChemRxiv. **License:** CC BY 4.0

and Bacillus Subtilis. *Environ. Sci. Technol.* **2020**, *54* (10), 6185–6193. https://doi.org/10.1021/acs.est.0c01186.

(12) Liu, Z.; Dibaji, A.; Li, D.; Mateti, S.; Liu, J.; Yan, F.; Barrow, C. J.; Chen, Y.; Ariga, K.; Yang, W. Challenges and Solutions in Surface Engineering and Assembly of Boron Nitride Nanosheets. *Mater. Today* **2021**, *44* (April), 194–210. https://doi.org/10.1016/j.mattod.2020.11.020.

(13) Doğan, D.; Metin, A. Ü. Physicochemical and Biological Assessment of Boron Nitride Nanosheets-Reinforced Poly(2-Hydroxyethylmethacrylate) Composite for Biomedical Applications. *Mater. Today Commun.* **2022**, *33* (October). https://doi.org/10.1016/j.mtcomm.2022.104807.

(14) Wu, N.; Yang, W.; Li, H.; Che, S.; Gao, C.; Jiang, B.; Li, Z.; Xu, C.; Wang, X.; Li, Y. Amino Acid Functionalized Boron Nitride Nanosheets towards Enhanced Thermal and Mechanical Performance of Epoxy Composite. *J. Colloid Interface Sci.* **2022**, *619*, 388–398. https://doi.org/10.1016/j.jcis.2022.03.115.

(15) Yang, N.; Ji, H.; Jiang, X.; Qu, X.; Zhang, X.; Zhang, Y.; Liu, B. Preparation of Boron Nitride Nanoplatelets via Amino Acid Assisted Ball Milling: Towards Thermal Conductivity Application. *Nanomaterials* **2020**, *10* (9), 1–12. https://doi.org/10.3390/nano10091652.

(16) Tian, X.; Wu, N.; Zhang, B.; Wang, Y.; Geng, Z.; Li, Y. Glycine Functionalized Boron Nitride Nanosheets with Improved Dispersibility and Enhanced Interaction with Matrix for Thermal Composites. *Chem. Eng. J.* **2021**, *408* (August 2020). https://doi.org/10.1016/j.cej.2020.127360.

https://doi.org/10.26434/chemrxiv-2024-lqj0v **ORCID:** https://orcid.org/0000-0002-4821-795X Content not peer-reviewed by ChemRxiv. **License:** CC BY 4.0

(17) Li, X.; Ma, J.; Gao, Y.; Liu, X.; Wei, Y.; Liang, Z. Enhanced Atrazine Degradation in the Fe(III)/Peroxymonosulfate System via Accelerating Fe(II) Regeneration by Benzoquinone. *Chem. Eng. J.* **2022**, *427* (May 2021), 131995. https://doi.org/10.1016/j.cej.2021.131995.

(18) Pérez, D. J.; Doucette, W. J.; Moore, M. T. Atrazine Uptake, Translocation, Bioaccumulation and Biodegradation in Cattail (Typha Latifolia) as a Function of Exposure Time. *Chemosphere* **2022**, *287* (June 2021). https://doi.org/10.1016/j.chemosphere.2021.132104.

(19) de Albuquerque, F. P.; de Oliveira, J. L.; Moschini-Carlos, V.; Fraceto, L. F. An Overview of the Potential Impacts of Atrazine in Aquatic Environments: Perspectives for Tailored Solutions Based on Nanotechnology. *Sci. Total Environ.* **2020**, *700*. https://doi.org/10.1016/j.scitotenv.2019.134868.

(20) Li, J.; Wan, Y.; Li, Y.; Yao, G.; Lai, B. Surface Fe(III)/Fe(II) Cycle Promoted the Degradation of Atrazine by Peroxymonosulfate Activation in the Presence of Hydroxylamine. *Appl. Catal. B Environ.* **2019**, *256*, 117782. https://doi.org/10.1016/J.APCATB.2019.117782.

(21) Huang, M. Y.; Zhao, Q.; Duan, R. Y.; Liu, Y.; Wan, Y. Y. The Effect of Atrazine on Intestinal Histology, Microbial Community and Short Chain Fatty Acids in Pelophylax Nigromaculatus Tadpoles. *Environ. Pollut.* **2021**, *288*, 117702. https://doi.org/10.1016/J.ENVPOL.2021.117702.

(22) Karatas, O.; Gengec, N. A.; Gengec, E.; Khataee, A.; Kobya, M. High-Performance Carbon Black Electrode for Oxygen Reduction Reaction and Oxidation of Atrazine by

https://doi.org/10.26434/chemrxiv-2024-lqj0v **ORCID:** https://orcid.org/0000-0002-4821-795X Content not peer-reviewed by ChemRxiv. **License:** CC BY 4.0

Electro-Fenton Process. *Chemosphere* **2022**, *287* (P4), 132370. https://doi.org/10.1016/j.chemosphere.2021.132370.

(23) Dhiman, N.; Jasrotia, T.; Sharma, P.; Negi, S.; Chaudhary, S.; Kumar, R.; Mahnashi, M. H.; Umar, A.; Kumar, R. Immobilization Interaction between Xenobiotic and Bjerkandera Adusta for the Biodegradation of Atrazine. *Chemosphere* **2020**, *257*, 127060. https://doi.org/10.1016/j.chemosphere.2020.127060.

(24) Iovino, P.; Chianese, S.; Fenti, A.; Blotevogel, J.; Musmarra, D. An Innovative Approach for Atrazine Electrochemical Oxidation Modelling: Process Parameter Effect, Intermediate Formation and Kinetic Constant Assessment. *Chem. Eng. J.* **2023**, *474* (September), 146022. https://doi.org/10.1016/j.cej.2023.146022.

(25) Huang, Y.; Han, C.; Liu, Y.; Nadagouda, M. N.; Machala, L.; O'Shea, K. E.; Sharma, V. K.; Dionysiou, D. D. Degradation of Atrazine by ZnxCu1−xFe2O4 Nanomaterial-Catalyzed Sulfite under UV–Vis Light Irradiation: Green Strategy to Generate SO4[Rad]−. *Appl. Catal. B Environ.* **2018**, *221* (June 2017), 380–392. https://doi.org/10.1016/j.apcatb.2017.09.001.

(26) Huang, M. T.; Lu, Y. C.; Zhang, S.; Luo, F.; Yang, H. Rice (Oryza Sativa) Laccases Involved in Modification and Detoxification of Herbicides Atrazine and Isoproturon Residues in Plants. *J. Agric. Food Chem.* **2016**, *64* (33), 6397–6406. https://doi.org/10.1021/acs.jafc.6b02187.

(27) Luo, Q.; Yan, X.; Lu, J.; Huang, Q. Perfluorooctanesulfonate Degrades in a Laccase-Mediator System. *Environ. Sci. Technol.* **2018**, *52* (18), 10617–10626.

(28) Luo, Q.; Lu, J.; Zhang, H.; Wang, Z.; Feng, M.; Chiang, S. Y. D.; Woodward, D.; Huang,

https://doi.org/10.26434/chemrxiv-2024-lqj0v **ORCID:** https://orcid.org/0000-0002-4821-795X Content not peer-reviewed by ChemRxiv. **License:** CC BY 4.0

Q. Laccase-Catalyzed Degradation of Perfluorooctanoic Acid. *Environ. Sci. Technol. Lett.* **2015**, *2* (7), 198–203. https://doi.org/10.1021/acs.estlett.5b00119.

(29) Mu, Y.; Zhan, G.; Huang, C.; Wang, X.; Ai, Z.; Zou, J.; Luo, S.; Zhang, L. Dechlorination-Hydroxylation of Atrazine to Hydroxyatrazine with Thiosulfate: A Detoxification Strategy in Seconds. *Environ. Sci. Technol.* **2019**, *53* (6), 3208–3216. https://doi.org/10.1021/acs.est.8b06351.

(30) Shapir, N.; Mandelbaum, R. T. Atrazine Degradation in Subsurface Soil by Indigenous and Introduced Microorganisms. *J. Agric. Food Chem.* **1997**, *45* (11), 4481–4486. https://doi.org/10.1021/jf970423t.

(31) Krishnasamy, L.; Krishna, K.; Subpiramaniyam, S. Photocatalytic Degradation of Atrazine in Aqueous Solution Using La-Doped ZnO/PAN Nanofibers. *Environ. Sci. Pollut. Res.* **2022**, *29* (36), 54282–54291. https://doi.org/10.1007/s11356-022-19665-2.

(32) Majhi, D.; Das, K.; Mishra, A.; Dhiman, R.; Mishra, B. G. One Pot Synthesis of CdS/BiOBr/Bi2O2CO3: A Novel Ternary Double Z-Scheme Heterostructure Photocatalyst for Efficient Degradation of Atrazine. *Appl. Catal. B Environ.* **2020**, *260* (September 2019), 118222. https://doi.org/10.1016/j.apcatb.2019.118222.

(33) Rimola, A. Intrinsic Ladders of Affinity for Amino-Acid-Analogues on Boron Nitride Nanomaterials: A B3LYP-D2* Periodic Study. *J. Phys. Chem. C* **2015**, *31*, 17707–17717. https://doi.org/10.1021/acs.jpcc.5b04601.

(34) Goudarzi, S.; Kaur, J.; Eslami, R.; Kouhpour, A.; Kalinina, M.; Yousefi, N.; Zarrin, H. Laccase-Functionalized Hexagonal Boron Nitride-Coated Sponges for the Removal and Degradation of Anthracene. *ACS Appl. Nano Mater.* **2022**, *5* (3), 4493–4505.

https://doi.org/10.26434/chemrxiv-2024-lqj0v **ORCID:** https://orcid.org/0000-0002-4821-795X Content not peer-reviewed by ChemRxiv. **License:** CC BY 4.0

https://doi.org/10.1021/acsanm.2c00694.

(35) *Laccase | C44H69N11O20 | CID 3013170 - PubChem*. https://pubchem.ncbi.nlm.nih.gov/compound/Laccase (accessed 2023-11-16).

(36) Mehra, R.; Muschiol, J.; Meyer, A. S.; Kepp, K. P. A Structural-Chemical Explanation of Fungal Laccase Activity. *Sci. Rep.* **2018**, *8* (1), 1–16. https://doi.org/10.1038/s41598-018-35633-8.

(37) Liu, J.; Cai, Y.; Liao, X.; Huang, Q.; Hao, Z.; Hu, M.; Zhang, D.; Li, Z. Efficiency of Laccase Production in a 65-L Air-Lift Reactor for Potential Green Industrial and Environmental Application. *J. Clean. Prod.* **2013**, *39*, 154–160. https://doi.org/10.1016/j.jclepro.2012.08.004.

(38) Rodrigues, R. C.; Berenguer-Murcia, Á.; Carballares, D.; Morellon-Sterling, R.; Fernandez-Lafuente, R. Stabilization of Enzymes via Immobilization: Multipoint Covalent Attachment and Other Stabilization Strategies. *Biotechnol. Adv.* **2021**, *52* (July). https://doi.org/10.1016/j.biotechadv.2021.107821.

(39) Chapman, R.; Stenzel, M. H. All Wrapped up: Stabilization of Enzymes within Single Enzyme Nanoparticles. *J. Am. Chem. Soc.* **2019**. https://doi.org/10.1021/jacs.8b10338.

(40) Zhou, Y.; Yang, Z.; Zhou, R.; Zeng, B.; Liu, X.; Li, X.; Zhang, G. Peptide-Inspired One-Step Synthesis of Surface-Functionalized Fe3O4Magnetic Nanoparticles for Oriented Enzyme Immobilization and Biocatalytic Applications. *ACS Appl. Nano Mater.* **2022**, *5* (6), 8260–8270. https://doi.org/10.1021/acsanm.2c01346.

(41) Zhou, W.; Zhang, W.; Cai, Y. Enzyme-Enhanced Adsorption of Laccase Immobilized Graphene Oxide for Micro-Pollutant Removal. *Sep. Purif. Technol.* **2022**, *294* (March),

https://doi.org/10.26434/chemrxiv-2024-lqj0v **ORCID:** https://orcid.org/0000-0002-4821-795X Content not peer-reviewed by ChemRxiv. **License:** CC BY 4.0

121178. https://doi.org/10.1016/j.seppur.2022.121178.

(42) Homaei, A. A.; Sariri, R.; Vianello, F.; Stevanato, R. Enzyme Immobilization: An Update. *J. Chem. Biol.* **2013**, *6* (4), 185–205. https://doi.org/10.1007/s12154-013-0102-9.

(43) Yang, S.; Ding, J.; Zheng, J.; Hu, B.; Li, J.; Chen, H.; Zhou, Z.; Qiao, X. Detection of Melamine in Milk Products by Surface Desorption Atmospheric Pressure Chemical Ionization Mass Spectrometry. *Anal. Chem.* **2009**, *81* (7), 2426–2436. https://doi.org/10.1021/ac900063u.

(44) Lang, D. H.; Rettie, A. E.; Böcker, R. H. Identification of Enzymes Involved in the Metabolism of Atrazine, Terbuthylazine, Ametryne, and Terbutryne in Human Liver Microsomes. *Chem. Res. Toxicol.* **1997**, *10* (9), 1037–1044. https://doi.org/10.1021/tx9700811.

(45) Koroleva, O. V.; Zherdev, A. V.; Kulikova, N. A.; Koroleva, O. V.; Zherdev, A. V.; Kulikova, N. A. The Role of White-Rot Fungi in Herbicide Transformation. In *Herbicides, Physiology of Action, and Safety*; IntechOpen, 2015. https://doi.org/10.5772/61623.

(46) Mohanty, S. K.; Torkelson, A. A.; Dodd, H.; Nelson, K. L.; Boehm, A. B. Engineering Solutions to Improve the Removal of Fecal Indicator Bacteria by Bioinfiltration Systems during Intermittent Flow of Stormwater. *Environ. Sci. Technol.* **2013**, *47* (19), 10791–10798. https://doi.org/10.1021/es305136b.

(47) Vazirzadeh, A.; Jafarifard, K.; Ajdari, A.; Chisti, Y. Removal of Nitrate and Phosphate from Simulated Agricultural Runoff Water by Chlorella Vulgaris. *Sci. Total Environ.* **2022**, *802*. https://doi.org/10.1016/j.scitotenv.2021.149988.

https://doi.org/10.26434/chemrxiv-2024-lqj0v **ORCID:** https://orcid.org/0000-0002-4821-795X Content not peer-reviewed by ChemRxiv. **License:** CC BY 4.0

(48) Zhuang, Y.; Wen, W.; Ruan, S.; Zhuang, F.; Xia, B.; Li, S.; Liu, H.; Du, Y.; Zhang, L. Real-Time Measurement of Total Nitrogen for Agricultural Runoff Based on Multiparameter Sensors and Intelligent Algorithms. *Water Res.* **2022**, *210* (November 2021). https://doi.org/10.1016/j.watres.2021.117992.

(49) Fatemi, F. R.; Fernandez, I. J.; Simon, K. S.; Dail, D. B. Nitrogen and Phosphorus Regulation of Soil Enzyme Activities in Acid Forest Soils. *Soil Biol. Biochem.* **2016**, *98*, 171–179. https://doi.org/10.1016/j.soilbio.2016.02.017.

(50) Ismail, S.; Elsamadony, M.; Abdalla, M.; Ni, S. Q.; Tawfik, A. Stimulating the Fermentation Process of Industrial Food Waste via Nonionic Surfactant/Graphene Nanosheet Combined Supplementation. *ACS ES&T Eng.* **2022**, *2* (11), 2043–2057. https://doi.org/10.1021/acsestengg.2c00140.

(51) Xue, Y.; Zhang, Z. M.; Zhang, R. R.; Li, Y. Q.; Sun, A. L.; Shi, X. Z.; Chen, J.; Song, S. Aquaculture-Derived Distribution, Partitioning, Migration, and Transformation of Atrazine and Its Metabolites in Seawater, Sediment, and Organisms from a Typical Semi-Closed Mariculture Bay. *Environ. Pollut.* **2021**, *271*. https://doi.org/10.1016/j.envpol.2020.116362.

(52) Stradtman, S. C.; Freeman, J. L. Mechanisms of Neurotoxicity Associated with Exposure to the Herbicide Atrazine. *Toxics* **2021**, *9* (9). https://doi.org/10.3390/toxics9090207.

https://doi.org/10.26434/chemrxiv-2024-lqj0v **ORCID:** https://orcid.org/0000-0002-4821-795X Content not peer-reviewed by ChemRxiv. **License:** CC BY 4.0